



**HAL**  
open science

## A new generalized stochastic Petri net modeling for energy-harvesting-wireless sensor network assessment

Oukas Nourredine, Boulif Menouar, Eric Campo, Adrien van den Bossche

### ► To cite this version:

Oukas Nourredine, Boulif Menouar, Eric Campo, Adrien van den Bossche. A new generalized stochastic Petri net modeling for energy-harvesting-wireless sensor network assessment. *International Journal of Communication Systems*, 2023, 36 (11), 10.1002/dac.5505 . hal-04811927

**HAL Id: hal-04811927**

**<https://laas.hal.science/hal-04811927v1>**

Submitted on 29 Nov 2024

**HAL** is a multi-disciplinary open access archive for the deposit and dissemination of scientific research documents, whether they are published or not. The documents may come from teaching and research institutions in France or abroad, or from public or private research centers.

L'archive ouverte pluridisciplinaire **HAL**, est destinée au dépôt et à la diffusion de documents scientifiques de niveau recherche, publiés ou non, émanant des établissements d'enseignement et de recherche français ou étrangers, des laboratoires publics ou privés.

Public Domain

# A New Generalized Stochastic Petri Nets Modeling for Energy-Harvesting-WSNs Assessment

OUKAS Nourredine<sup>1,2</sup> | BOULIF Menouar<sup>1\*</sup> | Eric Campo<sup>3</sup> | Adrien van den Bossche<sup>4</sup>

<sup>1</sup>LIMOSE laboratory, M'Hamed Bougara University of Boumerdes, Independence Avenue, 35000, Boumerdes, Algeria.

<sup>2</sup>LIM laboratory, Department of computer sciences, Akli Mohand Oulhadj University of Bouira, Bouira, Algeria.

<sup>3</sup>LAAS-CNRS, University of Toulouse, CNRS, UT2J, Toulouse, France.

<sup>4</sup>IRIT-CNRS, University of Toulouse, CNRS, UT2J, Toulouse, France.

## Correspondence

OUKAS Nourredine, Department of computer sciences, Akli Mohand Oulhadj University of Bouira, Bouira, Algeria  
Email: n.oukas@univ-bouira.dz; noureddine.mag@gmail.com

## Present address

\*m.boulif@univ-boumerdes.dz

## Funding information

This paper proposes an energy-harvesting-aware model that aims to assess the performances of wireless sensor networks. Our model uses Generalized Stochastic Petri Nets to define a sensor-neighbors relationship abstraction. The novelty of the proposed formulation is taking into account several real-life considerations such as battery-over breakdowns, unavailability of neighbors, retrial attempts, and sleeping mechanism in a single model. We use TimeNet tool to simulate the network behavior in order to evaluate its performance throughout different formulas after it had reached its steady state. Finally, we present a case study featuring the different solar energy recovery capabilities of the vast Algerian territory. The aim is to show with the presented model how to determine the kind of resources to be acquired in order to cope with the sensor deployment project requirements. The proposed model allows us to ensure that the battery energy level of sensors deployed in Algiers province for example is almost equal to 80% for 100 messages per day and (one minute/ two minutes) for (awakening time/ sleeping time) ratio.

## KEYWORDS

wireless sensor network, energy harvesting, retrial system, sleeping mechanism, dependent breakdowns, GSPN modeling, performance evaluation

1  
2  
3  
4  
5  
6  
7  
8  
9  
10  
11  
12  
13  
14  
15  
16  
17  
18  
19  
20  
21  
22  
23  
24

## 1 | INTRODUCTION

Wireless Sensor Networks (WSNs) are now well-established as an effective solution to some challenging problems such as environmental conditions monitoring, border security, human health control and natural disaster relief operations [1, 2]. A WSN is a network of small devices called Sensor Nodes (SNs) that cooperatively operate to sense, collect, receive and send data to a base station (BS). Generally, SNs communicate with the BS via a multi-hops path. That is, due to limited broadcasting range, sent messages have to make their way from a sensor to another until reaching the BS. In order to implement such networks, several considerations must be addressed, such as the type of sensors to use, SN size and dimension, sensing modalities, computation, communication and storage capabilities, cost, type of power source, deployment architecture, communication protocol, application and management tools [3]. Furthermore, WSNs are subject to breakdowns stemming in most cases from battery over [4, 5]. Indeed, the sensors have limited battery capacity, and hence, SNs can only operate for a limited period of time [6, 7].

An efficient solution that has been applied to deal with this problem is to use energy harvesting (EH). EH consists of equipping SNs with special components that enable them to get energy from their environment. Energy sources may have different forms such as sunlight, wind, wave, heat, foot strike, finger strokes and others. Depending on the periodicity and amount of the harvested energy, SN parameters must be adjusted in order to have a good compromise between decent performance and long lifetime. For example, a node can increase its sampling frequency or its duty cycle to enhance its sensing reliability, or it can increase the transmission power to reach more far neighbors, and hence decrease the length of the multi-hops routing path. However, this can negatively impact the node lifetime, or even the overall network.

To find such a compromise, these systems need to be evaluated before their actual implementation. Two approaches can be used to analyse a WSN behaviour [8]. The first one uses simulation software, whereas the second resorts to formal modeling. Despite being related, these approaches have quite different requirements. For example, when a researcher introduces a new WSN protocol of communication, he can conduct his assessment according to both approaches. However, by opting for the first method, the researcher must encode the new algorithms in the language of the simulation framework [8, 9]. Therefore, coding difficulties and long simulation time issues must be addressed. In addition to that, the researcher must be aware that the simulation environment can significantly affect the obtained results. However, the simulation provides platform-dependent results [8].

In the other hand, using mathematical modeling tools, such as Petri nets, allows high level of abstraction, thus providing platform-independent results [10]. In addition, besides the solid mathematical basis results are built upon, many of the real conditions features of the modeled systems can be represented.

Due to the power of GSPN modeling capabilities the present work proposes a formulation for evaluating the performances of EH-WSNs, by taking into account a set of factors that, to the best of our knowledge, have not been previously considered simultaneously. In fact, this paper handles the following aspects:

- It introduces a new modeling by using the GSPN formalism that includes simultaneously a set of SN features, and a number of WSN deployment conditions. On one hand, the features include (1) energy harvesting from the ambient to recharge the batteries, (2) network connectivity operations, and (3) a sleeping mechanism. On the other hand, the deployment constraints comprehend the representation of (1) retrial attempts, (2) breakdowns, and (3) repairs.

- 66 • It uses the quantization principle in order to incorporate battery charging and discharging processes.
- 67 • It adopts the famous "dependent breakdowns strategy" that procures a general framework for breakdown man-  
68 agement.
- 69 • It integrates an intelligent sleeping mechanism proposed in some recent works [11, 12] that enables saving energy  
70 when the harvesting rate declines. In the opposite situation, it permits speeding up the system response time. We  
71 integrate this mechanism for both main sensor and its neighbors in the modeled sensor-neighbors relationship to  
72 represent the unavailability of neighbors
- 73 • It presents a quantitative analysis that calculates several performance criteria. Then, by means of many examples,  
74 it shows the impact of some input values on the performance measures.
- 75 • It presents an actual case study for the deployment of WSNs in various Algerian territories. The study shows  
76 how the presented work can help to determine the appropriate SN features that allow to cope with the network  
77 deployment zone characteristics.
- 78

79 The rest of this paper is organized as follows: In Section 2, we present some related works. Next, in section 3,  
80 we describe the GSPN formalism. Section 4 describes the energy harvesting capabilities and explains the abstraction  
81 of EH-WSN by a sensor-neighbors relationship. In section 5, we develop a GSPN model for EH-WSN and we define  
82 several performance parameters' formulas. Section 6, which is devoted to the numerical results, starts by describing  
83 TimeNet tool. Then, it presents a case study. At the end of this section, we present and discuss the numerical results.  
84 Finally, we give our conclusion as well as our recommendations for future works.

## 85 2 | RELATED WORKS

86 Broadly speaking, using Petri nets to model network related problems has been adopted for a long time. Shojafar et al.  
87 [13] proposed a new three-tiered approach to solve the resource scheduling problem in grid computing environments  
88 using hierarchical stochastic Petri nets. Resource requests are categorized into layers. Each layer has specific tasks  
89 for receiving sub-tasks from and delivering data to the layer above or below. In [14], the authors presented what they  
90 called ALATO, which is an intelligent algorithm based on learning automata and adaptive stochastic Petri nets. In [15],  
91 Farooq et al. have proposed an approach based-on colored Petri nets to calculate random path routing in WSNs. In  
92 satellite networks, two Stochastic Petri Nets models are proposed to analyze the performance of satellite networks  
93 in traditional and active defense states [16].

94  
95 For WSN related works, several researchers resorted to Petri nets as a modeling tool for evaluating the perfor-  
96 mances of these networks. In [17], the authors proposed a colored Petri net to model and evaluate the performances  
97 of a medium access control (MAC [4]) protocol they called S-MAC. S-MAC uses a sleeping mechanism with rendezvous  
98 scheduling. They analyzed energy consumption when such a protocol is used. However, the authors did not consider  
99 the energy harvesting nor the eventuality of breakdowns.

100  
101 The authors of [18], proposed a Petri net to predict energy consumption by considering a sleeping mechanism  
102 to build the energy plan. They called the information on the residual power available in each part of the network:  
103 the power map. They use the GSPN formalism to model a route in WSN. First, they simplify the whole network by  
104 considering a point-to-point route with multiple hops. Then, they reduced the modeled route to a single hope taking

105 into account a node-to-node relationship. They predict the energy using the speed of each node of the considered  
106 hope. However, they considered a simple sleep mechanism with only two states. The transition between states is  
107 based on probability only. Therefore, it will be better to model the node battery and link the transition between the  
108 sensor's states at the battery level. Additionally, they neither considered failures, retrial attempts, nor the sleeping  
109 mechanism based on the battery level. Also, it is adequate to consider several neighbors for the next hop instead of  
110 one.

112 Yadollah et al. [19] presented an analytical modeling method that uses Petri nets for energy consumption as-  
113 sessment. The proposed model leads to the construction of a formal model based on GSPN to evaluate the power  
114 consumption of sensors in an S-MAC-based WSN. The conducted experiments deal with the number of nodes, duty  
115 cycle rate, upper-layer data flow, and packet size.

116 Lacerda et al. [20] proposed a GSPN framework to mimic the behavior of WSN with multi-hops topology. They in-  
117 vestigated the aggregation of similar packets in intermediate nodes, and its impact on the serving time of the whole  
118 network.

119 Zairi et al. [21] proposed a colored Petri net to study energy consumption of MAC protocols. They built what they  
120 called CP-NET to analyze the behavior of WSNs. The proposed framework allows protocol constructors to predict  
121 the behavior of the network, but the proposed approach didn't consider energy harvesting, nor breakdown/repair  
122 aspects.

123 Bechar et al. [22] proposed an approach for modeling and verifying the consistency and correctness of WSN protocols  
124 by using colored Petri net. They used a formal method based on the Event-B method. In the first step, the Petri net  
125 is used to elaborate network layer models, then, each one of them is detailed by an Event-B formalism.

126 In the WSN literature, there are works that take into consideration retrial phenomenon while considering sensor un-  
127 reliability, as in S. Zhang-Song et al. [18]. The authors proposed a GSPN model to predict energy consumption by  
128 considering a new sleeping mechanism to construct the energy plan. The sleeping mechanism is also considered in  
129 [23], where the authors proposed a Markov Chain model for energy-efficient sensor nodes.

130 Berczes et al. [24] introduced a finite source retrial queuing model to study the characteristics of transmission in  
131 WSNs. They considered two classes of sensors: one for special requests with high priority (used for alert), and the  
132 second for normal requests (to transmit data).

133 Wuchner et al. [25] presented the concept of unreliable orbit, and by using a GSPN model they evaluated the perfor-  
134 mance of WSNs. Their approach were based on a sensor-neighbors relationship.

135 Gharbi and Charabi [26] proposed an algorithmic approach based on GSPN formalism aiming at modeling and analyz-  
136 ing finite-source wireless networks with retrial phenomenon and two server classes.

137 Boutoumi and Gharbi [27] proposed the two thresholds working vacation policy, which is an energy saving and latency  
138 efficiency approach constructed over a GSPN model for full-duplex WSNs.

140 WSNs performance is closely related to the amount of energy stored in the SNs' batteries. Therefore, studying  
141 the factors that affect the energy consumption of a sensor while it is interacting with the rest of the network procures  
142 a key view on how the whole system is performing. Among these factors, we have the surrounding conditions that  
143 must be available to reach a certain network lifetime, the type of batteries to acquire, the mechanism of energy conser-  
144 vation to use, or the response time that can be obtained. Therefore, several works adopted such a sensor-neighbors  
145 relationship to evaluate WSNs.

146 For instance, the authors in [28] presented a Petri-net model that considered an SN equipped with a solar-energy  
147 harvester. They used the sensor-neighbors relationship to evaluate the system in terms of response time and amount

148 of energy stored in rechargeable batteries. The energy is represented by using the quantization principle. The model  
 149 incorporates mechanisms for power consumption in packet sending/receiving, monitoring, and processing. The au-  
 150 thors also considered battery recharging and a switching mechanism between energy-saving (sleep) and active modes.  
 151 The results obtained through the quantitative analysis made it possible to predict the average energy level of the SNs.  
 152 However, the work didn't consider the intermittent nature of the charging source (i.e. the sun).  
 153 The same authors proposed an energy conservation system based on an intelligent sleeping mechanism they called  
 154 DSM (dual sleeping mechanism) [29]. The presented study dealt with the absence of sunlight at night. Afterward, the  
 155 model of [28] was improved by considering the case of a long-lasting WSN deployment [30]. In this latter, the authors  
 156 considered the variable amount of energy that can be collected in each season.  
 157 More recently, the work presented in [11] combined the previous two considerations into a single model. That is the  
 158 seasonal sunshine levels and the succession of day and night.

159

160 Besides, several works considered other factors that can affect energy consumption, such as the distance sepa-  
 161 rating the receivers and the transmitters [31] and the differences in message lengths [32].  
 162 However, the works presented in [28], [30], [11] and [29] ignored several real-life circumstances such as the ability  
 163 to achieve retrial attempts, and the possibility of breakdowns. Furthermore, the collected energy was limited to only  
 164 one type, namely solar energy.

**TABLE 1** Related works features.

(EH: Energy harvesting, RA: Retrial attempts, SM: Sleeping mechanism, B: Breakdowns,  
 PL: Packet length, ND: Neighbor distance, NA: Neighbor Availability, PP: Packet Priority,  
 DV: Different Sensor Velocities, ME: Mean Energy, L: Latency, TU: Transceiver Utilization)

Ref.	Year	Constraints									Metrics			Case Study
		EH	RA	SM	B	PL	ND	NA	PP	DV	ME	L	TU	
[17]	2009	×	×	√	×	×	×	×	×	×	√	×	×	√
[25]	2010	×	√	√	×	×	×	×	×	×	×	√	×	×
[26]	2012	×	√	×	×	×	×	×	×	√	×	√	×	×
[24]	2013	×	×	×	√	×	×	×	√	×	×	√	×	×
[27]	2018	×	√	√	×	×	×	×	×	×	×	√	×	×
[28]	2019	√	×	√	×	×	×	×	×	×	√	√	×	×
[32]	2020	√	×	√	×	√	×	×	×	×	×	×	×	×
[31]	2020	√	×	√	×	×	√	×	×	×	√	×	×	×
[19]	2020	×	×	√	×	×	×	×	×	×	√	×	×	√
[29]	2022	√	×	√	×	×	×	×	×	×	√	√	×	×
[11]	2022	√	×	√	×	×	×	×	×	×	√	√	√	√
[33]	2022	√	√	√	√	×	×	×	×	×	√	√	×	×
Proposal	2022	√	√	√	√	×	×	√	×	×	√	√	√	√

165

166 In order to address these shortcomings, the study presented in [33] took into account the effect of breakdowns  
 167 and retriail attempts on energy level and response time. The proposed approach was intended to cope with the re-  
 168 quirements of a deployment area where breakdowns are very likely to happen, such as in military projects. This makes  
 169 it only suitable for limited and specific applications.

170  
 171 This paper proposes a GSPN model that aims at combining many of the before-mentioned factors (see Table 1  
 172 for the main features of our proposal in comparison to others). In facts, our model takes into account, simultaneously,  
 173 and for the first time to the best of our knowledge, the following considerations:

- 174 • a retriail strategy to cope with message losses,
- 175 • an intelligent sleeping mechanism to save energy.
- 176 • the dependent-failures strategy (see section 4.1 for further details),
- 177 • repairs of breakdown sensors to make them operational again.
- 178 • the model can be set up for any type of energy source, and any communication density (daily number of exchanged  
 179 packets), and any type of rechargeable batteries (in terms of capacity).

### 180 3 | GSPN FORMALISM

181 Petri nets (PN) are a graphical mathematical tool for modeling dynamic systems in order to analyze and evaluate their  
 182 behavior [34, 35]. More precisely, a PN is a bipartite digraph with two kinds of vertices: places and transitions. Places  
 183 are represented by circles and can contain marks (or tokens) represented by big dots. The arcs of a PN cannot connect  
 184 two vertices of the same kind. A transition can be fired if and only if its initial place has at least one mark. By assuming  
 185 only arcs with unary multiplicity, the firing consumes one token from each initial place (input place) and delivers one  
 186 token to each terminal place (output place).

187  
 188 Generalized stochastic Petri nets (GSPNs) are an extension to PNs that are well-fitted to systems that, in addition  
 189 to being distributed and asynchronous, are stochastic [36]. In a GSPN, there are two kinds of transitions: immediate  
 190 transitions (represented by thin black bar) which do not need a time to fire, and timed transitions (usually represented  
 191 by boxes) which describe the execution of an activity that requires a time to finish. In addition, GSPNs introduce a  
 192 special type of arcs called inhibitor arc (denoted by a solid circle head) which is intended to reverse the firing condition.  
 193 That is, the associated transition can fire if there is no tokens in the input place.

194 Formally, a GSPN is an eight-tuple  $(P, T, \Pi, I, O, H, W, M_0)$  where:

195  $P$  is the set of places.

196  $T$  is the set of transitions such that  $P \cap T = \emptyset$ .

197  $\Pi: T \rightarrow \mathbb{N}$ , is the priority function which associates the priority  $\Pi(t) = n$  to an immediate transition, and  $\Pi(t) = m$   
 198 to a timed transition, ( $n, m \in \mathbb{N}$  and  $n > m$ ).

199  $I: S_1(P \times T) \rightarrow \mathbb{N}$ , is a function such that  $S_1(P \times T)$  is the set of non inhibitor arcs and  $I((p, t))$  defines the  
 200 multiplicity of the (input) arc  $(p, t)$  which connects the place  $p$  to the transition  $t$ .

201  $O: S_2(T \times P) \rightarrow \mathbb{N}$ , is a function such that  $O((t, p))$  determines the multiplicity of the (output) arc  $(t, p)$  that  
 202 connects the transition  $t$  to the place  $p$ .

203  $H: S_3(P \times T) \rightarrow \mathbb{N}$ , is a function that associates the multiplicity to each element of the set of inhibitor arcs  
 204  $S_3(P \times T)$ .

205  $S_1(P \times T) \cup S_2(T \times P) \cup S_3(P \times T)$  forms the set of existing arcs.

206  $W : T \rightarrow \mathbb{R}^*$ , is a function that associates a firing rate to each timed transition and a weight to each immediate  
207 transition.

208  $M_0 : P \rightarrow \mathbb{N}$ , is a function which associates to each place  $p$  the initial number of marks  $M_0(p)$ .

209 The system state is described by means of markings. A marking at an instant  $i$  is described by the vector  $M_i =$   
210  $(M_i(p_1), M_i(p_2), \dots, M_i(p_{|P|}))$ , such that  $M_i(p)$  gives the number of tokens in the place  $p$  at the instant  $i$ . Starting  
211 from the initial state  $M_0$ , the dynamic behavior of the GSPN results from the different markings that are obtained  
212 from the firing of the transitions.

213 A transition  $t$  fires in a marking  $M_i$  if and only if:

$$214 \forall (p, t) \in S_1(P \times T), M_i(p) \geq I((p, t)) \wedge \forall (p, t) \in S_2(P \times T), M_i(p) < H((p, t)).$$

215 Hence, a new marking can be defined for every place  $p$  linked to  $t$  as follows:

$$216 \forall (p, t) \in S_1(P \times T) : M_{i+1}(p) = M_i(p) - I((p, t)), \text{ and}$$

$$217 \forall (t, p) \in S_3(T \times P) : M_{i+1}(p) = M_i(p) + O((p, t))$$

218 The reachability graph of the GSPN is directed. The vertices are the overall markings that can be directly or indi-  
219 rectly reached from the initial state. Arcs are defined by the direct reachability relation and labelled by the correspond-  
220 ing transitions and take as weight the timed transition rates leading to the infinitesimal generator of the associated  
221 Markov chain. So, numerous results can be obtained using classical Markov chain theory [37].

222 The first step in the steady state analysis is study of ergodicity i.e. the existence and unicity of a finite steady  
223 state probability distribution [38]. If a GSPN is ergodic (bounded GSPN with strongly connected reachability graph),  
224 then there is a unique solution for the steady state probability distribution of the associated continuous time Markov  
225 chain. The resolution of the following linear system yields the solution of the steady state:

$$\begin{cases} \pi \cdot A = 0 \\ \sum \pi_i = 1 \end{cases}$$

226 such that  $A$  is the infinitesimal generator matrix, and  $\pi$  is the vector of steady state probability distribution of the  
227 associated continuous Markov chain [35].

228

229 From the equilibrium distribution, several steady state performance parameters can be computed such as: the  
230 mean number of tokens per place, the mean sojourn time in a place, the meantime spent in a set of markings, the  
231 resource utilisation ratio and others [37].

## 232 4 | DESCRIPTION OF EH-WSNS

### 233 4.1 | Energy harvesting considerations

234 In comparison to WSN, an EH-WSN node includes an additional component called energy harvesting unit responsi-  
235 ble of converting energy from environmental sources to electricity (see Figure 1). The power management module  
236 collects electrical energy from the harvester to directly supply it to the node or it may be stored in a storage module  
237 for future usage [1].

238

239 Hence, energy harvesting can be divided into two architectures (see Figure 2): Harvest-Use and Harvest-Store-  
240 Use architectures [3]. The second variant, we consider hereafter, can be implemented according to two alternatives



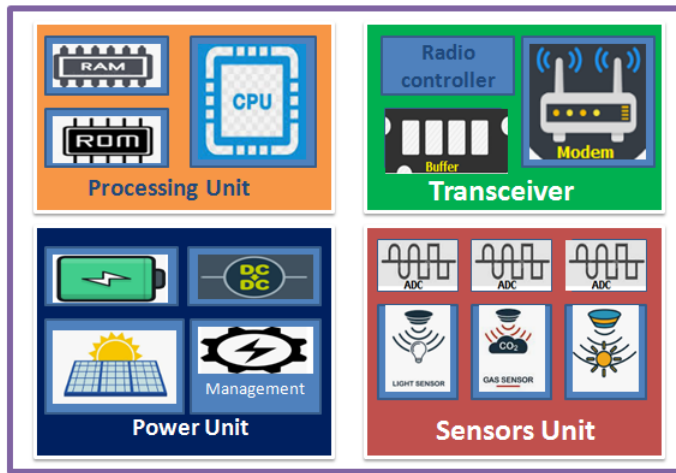


**FIGURE 1** A sensor node with an energy harvesting subsystem [11]

241 that are commonly used for energy storage: secondary rechargeable batteries and super-capacitors. For further de-  
 242 tails, we refer the readers to [1].

243

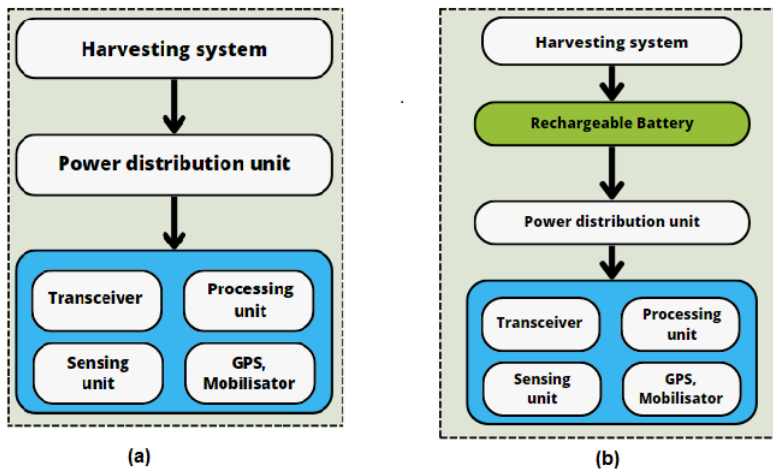


**FIGURE 2** Different architectures of harvesting system; (a): Harvest-use architecture; (b): Harvest-store-use architecture

244 Furthermore, to choose an energy harvesting system from various possible sources, one of the main criteria is to  
 245 determine whether or not it can provide the required power level for the sensor node [39]. Solar energy is an afford-  
 246 able and clean energy source that could alleviate or eliminate the energy shortage problem in WSNs. Photovoltaic  
 247 energy conversion is a traditional and well established energy-harvesting technology. It provides higher power out-

248 put levels compared to other energy harvesting techniques, and is suitable for large-scale energy harvesting systems.  
 249 Its generated power and the system efficiency strongly depends on the availability of light and on environmental  
 250 conditions [3][1], two conditions that are broadly available for our case study (see section 5.2).

251 Another aspect that is more or less related to energy is the breakdowns occurrence. Indeed, breakdowns generally  
 252 occurs due to battery exhaustion [40, 6, 7] which generally stems from an unsuitable energy-harvesting rate. In the  
 253 literature, we can find different policies of breakdowns such as active and independent breakdowns disciplines. The  
 254 interested reader can refer to [41, 42] for more details. In our work, we focus on the dependent breakdowns discipline  
 255 as described by Gharbi and Ioualalen [43], where the failure probability depends on the sensor state. I.e. the failure  
 rates of an active sensor and an idle one are not necessarily equal (see Figure 3).

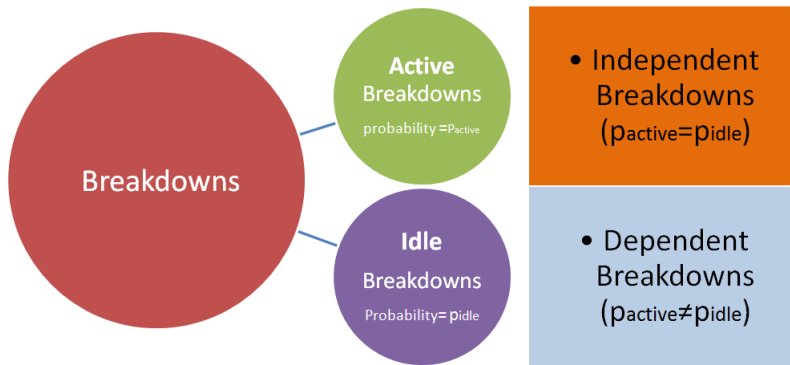


FIGURE 3 Breakdowns strategies

256

## 257 4.2 | Abstraction of EH-WSN by a sensor-neighbors relationship

258 In order to analyze the WSN behavior, we adopt an approach based on modeling the communication between a sensor  
 259 and its neighbors [25]. A neighbor is a sensor that can be reached in one hop in the message delivery path to the base  
 260 station.

261 The sending sensor node, we call the main sensor, senses incidents from the vicinity, and then tries to deliver a report  
 262 to the base station by sending a message to an idle neighbor (Figure 4). The main sensor can also receive messages  
 263 from its neighbors and takes care to forwarding them further to the sink. So, a message to be sent can be initiated by  
 264 the main sensor itself or from neighboring hops.

265 In our model, we suppose that all the sensors are identical. Any sensor can be in operational or down state. It can  
 266 be in an awake or sleeping state, and it can be idle or busy (see Figure 5).

267 The messages arrive to the main sensor who attempts to send them. If it has at least one idle neighbor, the  
 268 message sending starts immediately towards one randomly chosen neighbor. When the sending process terminates,  
 269 the receiver node becomes idle. When the main sensor fails to send a message to any of its neighbors, it stores it  
 270 locally in order to retry forwarding it later. In this case, the message is considered to be in orbit. While the main sensor  
 271 is on duty, it is subject to energy over. Energy harvesting capability may postpone this crippling situation, or it may  
 272 enable the sensor to resume when it is down. In what follows we enumerate the parameters that govern our model.

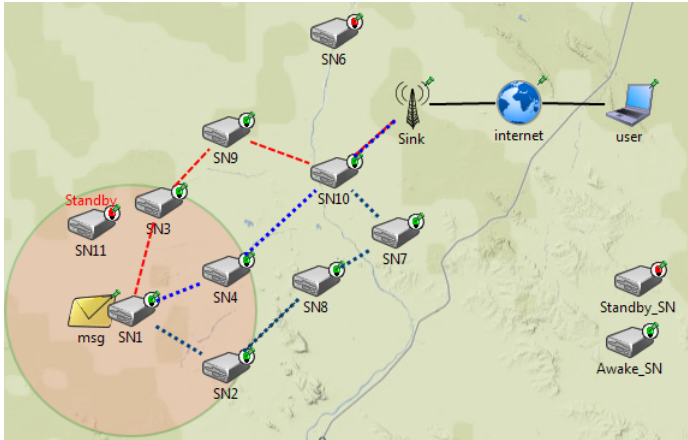


**FIGURE 4** A sensor node and its neighbors in WSNs

273 We suppose that the number of messages is finite and that it is not greater than  $N$ . The number of neighbors is  $s$ .  
 274 Messages arrive at each sensor node with a rate  $\lambda$ . Message-sending requests are randomly assigned to idle neighbors.  
 275 Sending times are assumed to be independent and exponentially distributed with a rate  $\mu$ . The time interval between  
 276 every two consecutive attempts is assumed to be exponentially distributed with a rate  $\nu$ .

277 A neighbor can be idle or busy. In both of these states, a breakdown event can occur involving the neighbor falling  
 278 in a down state. The breakdowns of the neighbors are assumed to be independent and exponentially distributed. If the  
 279 neighbor is idle, the breakdown rate associated with the exponential distribution is  $\delta$ ; whereas it is  $\gamma$  if the breakdowns  
 280 occur in the busy state.

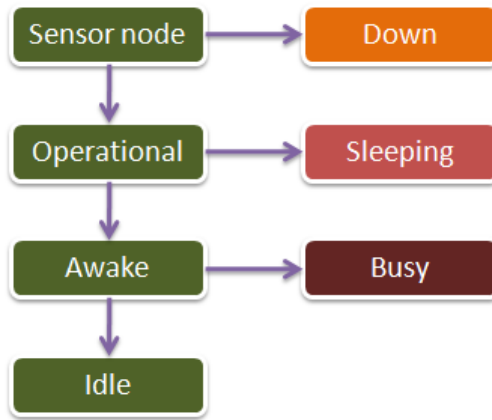


**FIGURE 5** Sensor node states

281 **5 | GSPN MODEL FOR EH-WSN**

282 **5.1 | Description**

283 In this subsection, we propose a Petri net model to evaluate and analyze the performance of EH-WSNs.

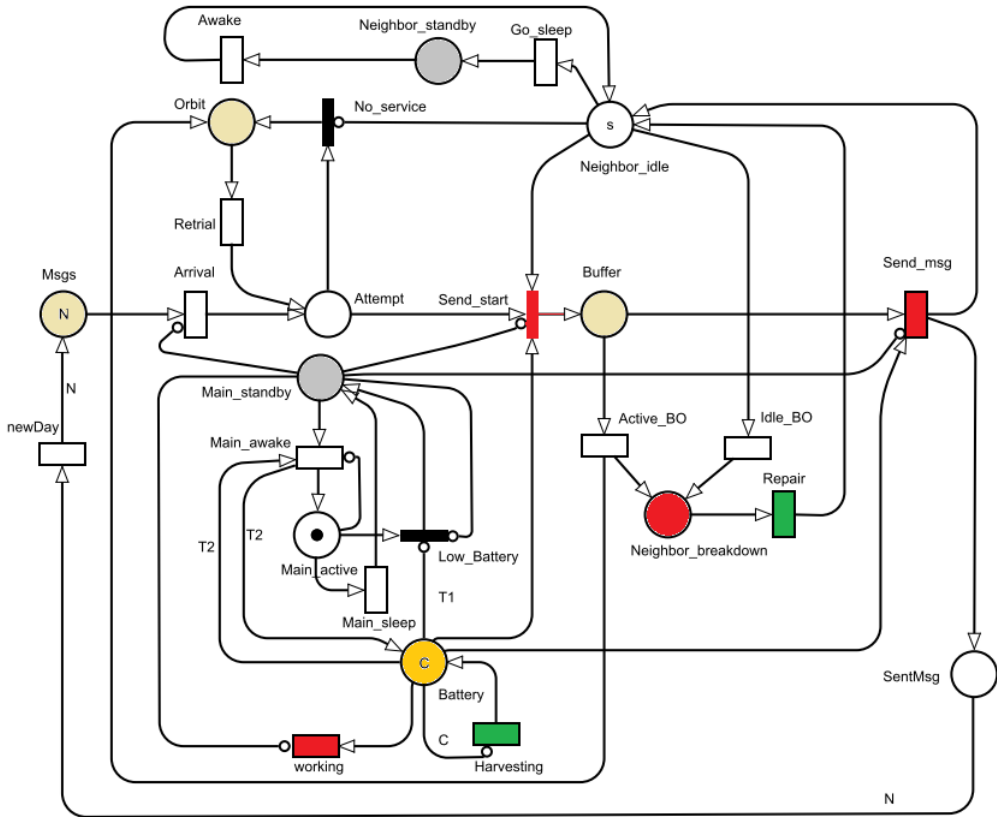


**FIGURE 6** GSPN model for EH-WSN with repeated attempts and sleeping mechanism

284 Figure 6 represents our GSPN model that takes into account repeated attempts, sleeping mechanism, dependent  
 285 breakdowns, repairs, battery exhaustion, and energy harvesting. The place *Msgs* contains the messages to be  
 286 sent by the main sensor. The place *Attempt* represents the arrival of an incident report, a received message, or  
 287 a retrial attempt for sending. Each token in the place *Orbit* represents a retrial attempt to send a message. Each  
 288 token in the place *Neighbor\_idle* represents an idle neighbor. Initially, there are *s* tokens in this place. The place  
 289 *Neighbor\_standby* represents sensor neighbors in sleeping state. Tokens in the place *Buffer* represent messages  
 290 in a sending phase. The place *Neighbor\_breakdown* contains neighbors in down state.  
 291 If a message arrives to the place *Attempt* and finds an idle active neighbor, it enters directly to the sending service, be-  
 292 cause *Send\_start* is an immediate transition. If there is no available neighbor (i.e. the place *Neighbor\_idle* is empty)  
 293 or the main sensor is in the sleeping state (i.e. there is a token in the place *Main\_standby*), the message joins the orbit  
 294 in order to repeat its attempts later. The firing of the transition *Send\_msg* represents a successful message sending.

**TABLE 2** Timed transitions description

Index	Transition	Signification	Firing rate
1	<i>Arrival</i>	Arrival of a message to the main node	$\lambda$
2	<i>Send_msg</i>	Transceiver sends a message	$\mu$
3	<i>Retrial</i>	Retry to send a message	$\nu$
4	<i>Idle_BO</i>	Failure of an idle neighbor	$\delta$
5	<i>Active_BO</i>	Failure of a busy neighbor	$\gamma$
6	<i>Repair</i>	Repair of neighbors	$\alpha$
7	<i>Go_sleep</i>	A neighbor goes to standby state	$\theta$
8	<i>Awake</i>	A neighbor awakes	$\omega$
9	<i>Main_sleep</i>	Main sensor to standby	$\theta$
10	<i>Main_awake</i>	Main sensor to awake	$\omega$
11	<i>Harvesting</i>	Energy harvesting process	$H_r$
12	<i>working</i>	Regular Energy consumption	$W_r$
13	<i>newDay</i>	Initializes the model each 24 hours	$I_r$

Two tokens will be generated, one represents the liberation of a sensor neighbor and joins the place *Neighbor\_idle*; whereas the second joins the place *Msgs* as an idea to preserve the model aliveness.

297

In order to save energy, sensor neighbors join the standby state with a rate  $\theta$ . After a certain time, the transition *Awake* is fired with a rate  $\omega$ . In addition, the main sensor joins the sleeping state by firing the *Main\_sleep* transition periodically. We define two thresholds:  $T_1$  and  $T_2$ . When the level of battery energy is lower than  $T_1$ , it joins the sleeping state directly by firing the transition *low\_battery*. The SN awakes by firing the transition *Main\_awake* if the level of energy in the battery is greater than or equal to the threshold  $T_2$ .

303

Concerning energy considerations, the presence of a rechargeable battery is represented by the place *Battery* that initially contains  $C$  quanta of energy. The number of quanta increases when the transition *Harvesting* fires (see the green-colored transitions in the model), and it decreases when the main SN is active (see the red-colored transitions in the model). We suppose that sending or receiving one message to or from a neighbor consumes one quantum of energy.

Before the end of a message receiving, the receiver can break down due to battery over. This event triggers the *Active\_BO* firing that generates two tokens: one joins the place *Neighbor\_breakdown* and the second joins the place *Orbit* as a retrial of message sending. Note that if a sensor fails while being idle, a token will be produced by the transition *Idle\_BO* and will join the place *Neighbor\_breakdown*. Tables 2 and 3 describe timed-transitions and places respectively.

314

On the other hand, tokens can represent resources or conditions. In Table 3, we define the type of tokens a place can contain. For the energy modeling, each token in the place *Battery* represents a *quantum*. Hence, the energy stored in the battery corresponds to the number of tokens in the place *Battery*. For instance, if there is  $e$  tokens in that place, then the battery contains  $e$  quanta of energy. The maximum number of tokens the place *Battery* can store is called *capacity* and will be noted  $C$ .

320

321 The initial state of the model is described by the marking  $M_0$  such that:

- 322 •  $M_0(Msgs) = N$ ,
- 323 •  $M_0(Neighbor\_idle) = s$ ,
- 324 •  $M_0(Main\_active) = 1$ ,
- 325 •  $M_0(Battery) = C$  and
- 326 • 0 for the remainder places.

327 The GSPN model of Figure 6 is *bounded* and the reachability graph derived by the TimeNet tool is strongly  
 328 connected, so the model is ergodic and involves the existence of a unique solution for the steady-state probability  
 329 distribution of the associated continuous Markov chain.

**TABLE 3** Description of places

Index	Name	Description	Token type	Initial value
1	<i>Msgs</i>	Source of messages	message	$N$
2	<i>Buffer</i>	Main SN's buffer	message	0
3	<i>Orbit</i>	Orbit of the main SN	message	0
4	<i>Attempt</i>	A message attempting to get the service	message	0
5	<i>Battery</i>	Main SN's battery	quantum	$C$
6	<i>Main_active</i>	Main SN active	boolean	1
7	<i>Main_standby</i>	Main SN sleeping	boolean	0
8	<i>Neighbor_idle</i>	Idle neighbors	neighbor	$s$
9	<i>Neighbor_standby</i>	Busy neighbors	neighbor	0
10	<i>Neighbor_breakdowns</i>	Broken neighbors	neighbor	0
11	<i>SentMsg</i>	Sent messages	message	0

## 330 5.2 | Performance formulas

331 Having the steady-state probability distribution  $\pi$ , several formulas of performance measures and reliability indexes  
 332 of the system can be derived as follows [37, 43]:

- 333 • The mean number of busy neighbors  $\bar{n}_b$ . It corresponds to the mean number of marks in the place *Buffer*:

$$\bar{n}_b = \sum_{i: M_i \in M} M_i(Buffer) \cdot \pi_i \quad (1)$$

- 334 • The mean number of idle active neighbors  $\bar{n}_i$ . It corresponds to the mean number of marks in the place *Neighbor\_idle*:

$$\bar{n}_i = \sum_{i: M_i \in M} M_i(Neighbor\_idle) \cdot \pi_i \quad (2)$$

- 335 • The mean number of retrial messages  $\overline{n_o}$ . It corresponds to the mean number of marks in the place *Orbit*:

$$\overline{n_o} = \sum_{i:M_i \in M} M_i(Orbit) \cdot \pi_i \quad (3)$$

- 336 • The mean battery charge  $\overline{Battery}$ . It corresponds to the mean number of marks in the place *Battery*:

$$\overline{Battery} = \sum_{i:M_i \in M} M_i(Battery) \cdot \pi_i \quad (4)$$

- 337 • The mean number of all messages in the retrial system  $\overline{n}$ . It corresponds to the sum of mean number of marks in the place *Orbit* and the mean number of marks in the place *Buffer*:

$$\overline{n} = \overline{n_b} + \overline{n_o} \quad (5)$$

- 339 • The mean number of neighbors in the sleeping state  $\overline{n_s}$ . It corresponds to the mean number of tokens in the place *Neighbor\_standby*:

$$\overline{n_s} = \sum_{i:M_i \in M} M_i(Neighbor\_standby) \cdot \pi_i \quad (6)$$

- 341 • The mean number of neighbors in breakdown state  $\overline{n_f}$ . It corresponds to the mean number of marks in the place *Neighbor\_breakdown*:

$$\overline{n_f} = \sum_{i:M_i \in M} M_i(Neighbor\_breakdown) \cdot \pi_i \quad (7)$$

- 343 • The mean rate of message arrivals  $\overline{\lambda}$ . It corresponds to the debit of the transition *Arrival*:

$$\overline{\lambda} = \sum_{i:M_i \in M(arrival)} \lambda \cdot M_i(Msgs) \cdot \pi_i \quad (8)$$

- 344 • The mean rate of message retrials  $\overline{v}$ . It corresponds to the debit of the transition *Retrial*:

$$\overline{v} = \sum_{i:M_i \in M(Retrial)} v \cdot M_i(Orbit) \cdot \pi_i \quad (9)$$

- 345 • The mean rate to send a message  $\overline{\mu}$ . It corresponds to the debit of the transition *Send\_msg*:

$$\bar{\mu} = \sum_{i: M_i \in M(\text{Send\_msg})} \mu \cdot M_i(\text{Buffer}) \cdot \pi_i \quad (10)$$

- 346 • The mean rate of the awake  $\bar{\omega}$ . It correspond to the debit of the transition  $Be\_awake$ :

$$\bar{\omega} = \sum_{i: M_i \in M(\text{Awake})} \omega \cdot M_i(\text{Neighbor\_standby}) \cdot \pi_i \quad (11)$$

- 347 • The mean rate of sleeping  $\bar{\theta}$ . It corresponds to the debit of the transition  $Go\_sleep$ :

$$\bar{\theta} = \sum_{i: M_i \in M(\text{Go\_sleep})} \theta \cdot M_i(\text{Neighbor\_idle}) \cdot \pi_i \quad (12)$$

- 348 • The mean waiting time of a message  $\bar{W}$ . It corresponds to the time between the arrival and the send starting.  $\bar{W}$   
349 is calculated by the Little formula [37]:

$$\bar{W} = \frac{\bar{n}_o}{\lambda} \quad (13)$$

- 350 • The mean response time of a message  $\bar{R}$ . It corresponds to the time between the arrival and the sending end:

$$\bar{R} = \frac{\bar{n}}{\lambda} \quad (14)$$

## 351 6 | NUMERICAL RESULTS

### 352 6.1 | TimeNet tool

353 TimeNet is an interactive graphical toolkit that supports modeling problems with GSPNs [44]. It is specially tailored for  
354 the steady state analysis of stochastic Petri nets. In addition, it can be used to achieve a transient analysis. TimeNet  
355 is an alternative to deriving the underlying reachability graph, and to determining the steady-state solution manually.  
356 In addition, it provides a Master/Slave concept with parallel applications and techniques for monitoring the statistical  
357 accuracy as well as reducing the simulation time length.

358 Compared to other tools, TimeNet provides a variety of efficient qualitative and quantitative analysis algorithms.  
359 TimeNet's graphical user interface has been completely written in JAVA. We refer the interested reader to [44] for  
360 more details. Figure 7 illustrates the quantitative analysis steps when using TimeNet.



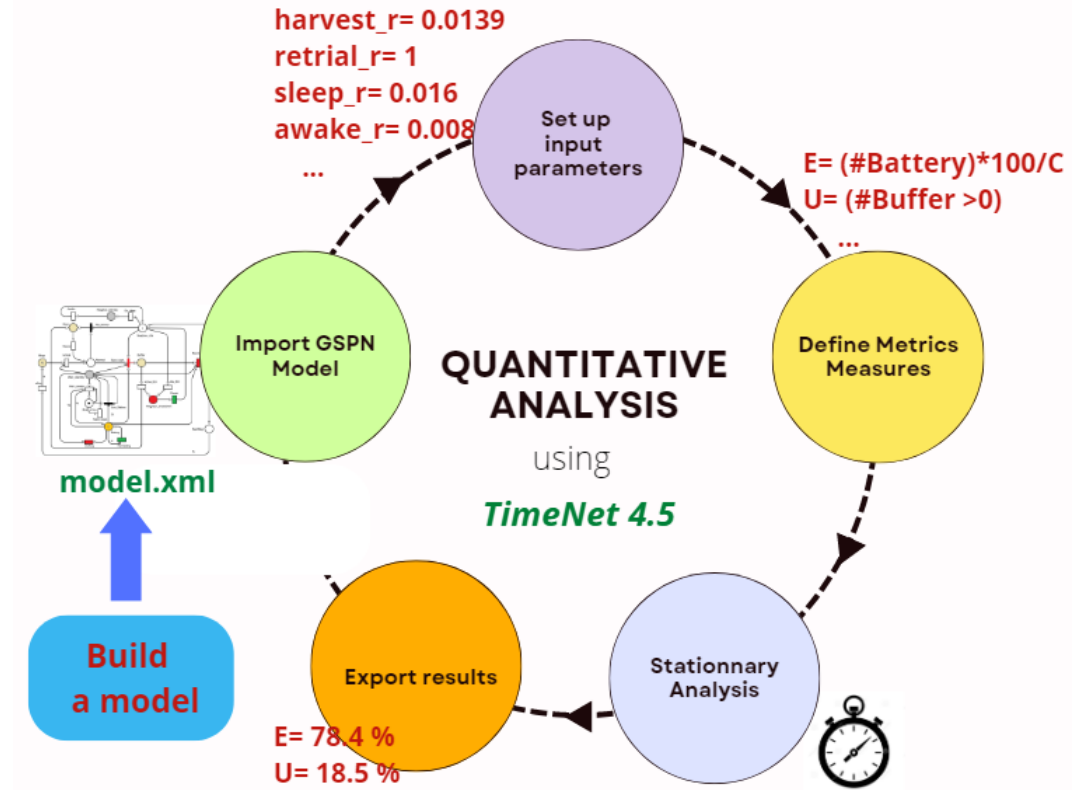


FIGURE 7 Example of a quantitative analysis of a GSPN by using TimeNet 4.5

## 361 6.2 | Performance analysis

362 TimeNet tool can compute various performance metrics. Table 4 contains the input values we used. The analysis is  
363 conducted by feeding the proposed model with different input values to experiment the network behavior for several  
364 scenarios.

365

366 We chose four performance metrics:

- 367 • Mean energy ( $E$ ),
- 368 • Mean response time ( $R$ ),
- 369 • Transceiver utilization ( $T$ ), and
- 370 • Repairer utilization ( $P$ ).

371 By following the syntax of TimeNet, these measures are defined as follows:

372  $E = (\#Battery) * 100 / C\%$

373  $R = ((\#Buffer) + (\#Orbit)) / ((\#Msgs > 0) * \lambda$

374  $T = (\#Buffer > 0) * (\#Main\_standby > 0) * 100\%$

$$P = (\#Neighbor\_breakdown > 0) * 100\%$$

376

377 Where:  $C$  is the initial number of marks in the place *Battery*, and  $\lambda$  is the arrival rate (see Table 2).

**TABLE 4** Input values for the analysis

Parameter	Value
Daily messages mean number ( $N$ )	100
Mean number of neighbors ( $s$ )	5
Sensor battery capacity ( $C$ )	100
$T1$	10%
$T2$	30%
Harvesting rate	2 quanta/s
Working rate	3 quanta/s
Retrial rate	20
Active breakdowns rate	$10^{-5}$
Idle breakdowns rate	$10^{-6}$
Repair rate	0.5
Sleeping rate	0.03
Awakening rate	0.6

### 378 6.2.1 | Influence of energy harvesting rate

379 Energy harvesting (EH) rate depends on the area where the network will be deployed. If the responsible of network  
 380 deployment has the choice between several areas with different harvesting rates, it can determine the suitable config-  
 381 uration for each area. By varying the energy harvesting rate and then monitoring the network behavior, we obtained  
 382 the following results:

383

384 Figure 8 illustrates the influence that EH has on the mean response time. When the EH rate increases (that is, the  
 385 time to harvest one quantum gets smaller), the mean response time decreases. We can notice that the mean response  
 386 time remains almost constant at the value 0.06 seconds until the harvesting rate reaches one quantum per second.  
 387 Then, it decreases from the value 10 to the value 100 reaching half of its initial value ( $\approx 0.03$ ).

388

389 Figure 9 shows the impact of EH on the mean battery charge. When the harvested-energy-per-second is less  
 390 than one quantum, the mean battery energy is almost stable around 30%, then, it starts to grow. When it reaches 10  
 391 quanta per second, the harvested energy rate is sufficient to maintain the amount of energy above one-half of full  
 392 capacity.

393

394 Figure 10 describes the utilization of the transceiver and the repairer versus the EH rate. The transceiver is the

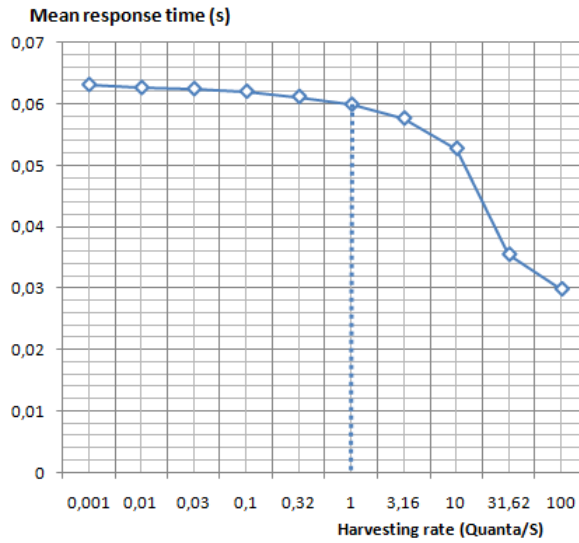


**FIGURE 8** Mean response time versus harvesting rate

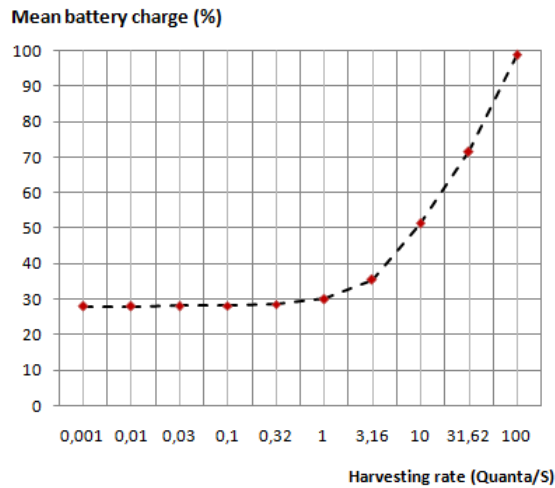


**FIGURE 9** Mean Battery charge versus harvesting rate

395 communication unit of the sensor node. It is responsible of receiving and sending messages (see the SN architecture  
 396 in Figure 1). The repairer represents the sensor maintenance function which is modeled in our GSPN by the presence  
 397 of the *Repair* transition. This function is supposed to be the duty of the harvesting system. Indeed, most of sensor  
 398 breakdowns stems from battery over (see subsection 3.1) and therefore, each reparation is done by recharging the  
 399 sensor's battery to let it leave the *Down* state. We notice that the utilization of both transceiver and repairer are  
 400 almost equal to zero when the harvesting rate is less than *one* quantum. In this case, the SN is on standby most of

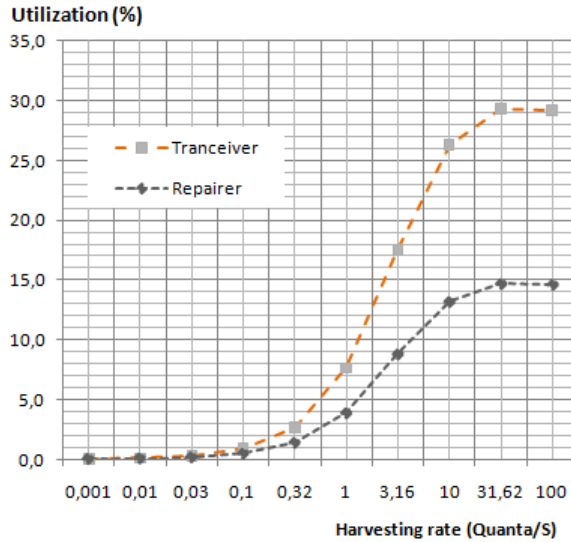


**FIGURE 10** Transceiver and repairer utilization versus harvesting rate

401 the time in order to preserve energy. As it is mentioned in the description of our proposed model, we defined two  
 402 thresholds  $T_1$  and  $T_2$ . If the energy becomes below  $T_1$ , the SN joins the sleeping state immediately, and it stays there  
 403 until the energy becomes equal or greater than  $T_2$  due to the EH. After that, the utilization increases until it reaches  
 404 the value 30% for the transceiver, and the value 15% for the repairer where they both stabilize.

405

406 In a nutshell, the last three figures depict the system behavior according to energy recovery from the ambient.  
 407 More energy is recovered involves fast message serving and good use of resources. For instance, if we choose a  
 408 deployment territory that permits to harvest more than 10 quanta per second, the level of battery charge will not  
 409 fall below 50%, and we will be using no more than 30% of the transceiver capability and 15% of the repairer to serve  
 410 messages in 0.04 second.

### 411 6.2.2 | Influence of Sleep/Awake ratio

412 Setting the sleep/Awake (SA) ratio is a key performance feature. Indeed, in order to save energy, an SN that was idle  
 413 for a long time requires to enter the sleep state. This will in addition enhance the efficiency of the harvesting process.  
 414 However, when sleeping, the SN misses calls from its neighbors, which will eventually require for them to do several  
 415 recalls before delivering their messages. Therefore, by following the same previous procedure, we can search for the  
 416 most suitable SA ratio.

417

418 Figure 11 shows the SA effect on the amount of energy stored in the SN battery. SA ratio induces the maximum  
 419 time an SN will stay listening. For example, a 0.03 sleeping rate means the SN will go to sleep if there is no message  
 420 to serve after one minute. We notice that the mean battery charge remains constant at 30% when the sleep/awake  
 421 ratio is below 0.03 (which means the sensor is active most of the time). After that, the mean charge grows until the  
 422 battery becomes fully charged (This happens when the SA ratio exceeds 10). In another hand, with a sleeping rate

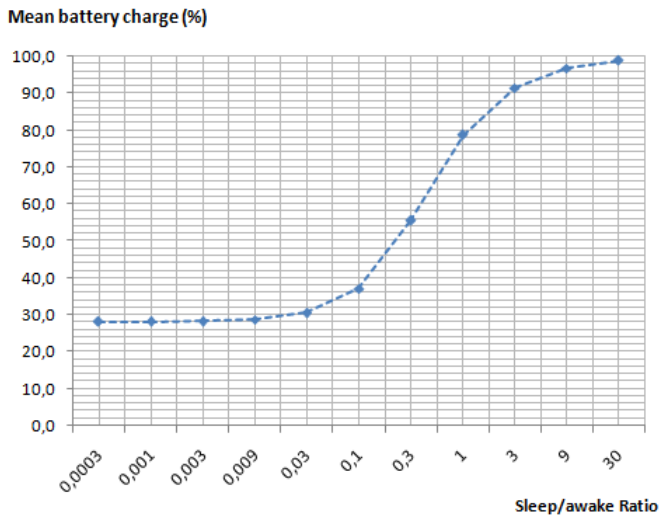


**FIGURE 11** Mean battery charge versus Sleep/Awake ratio

423 equal to 0.03 and an awaking rate equal to 0.003, we have an SA ratio equal to 10. With these values the mean energy  
 424 charge equals 98%. In this case, if the sensor enters the sleeping state, it will stay there for almost 6 minutes before  
 425 awaking. This configuration gives a mean response time equal to 0.61 second as it is depicted in Figure 12. Hence, if  
 426 such a performance does not fulfil the network duty requirement, and we seek for a faster one, we have to choose a  
 427 configuration that allows the sensors to stay active for a longer time.

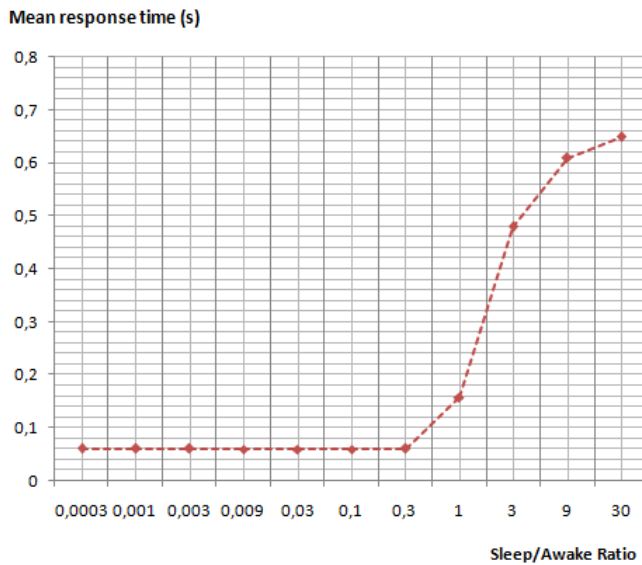


**FIGURE 12** Mean response time versus Sleep/Awake ratio

428 From Figure 12, we notice that the curve of mean response time has an inflexion point whose SA value is different  
 429 from 1. In fact, the vertical line that passes by 1 divides the curve into two parts: fast configuration (SN awakes most  
 430 of the time) and slow configuration (SN sleeps most of the time). Therefore, the gain in response time grows before  
 431 this edge value but slows at the value  $\approx 1.7$ .

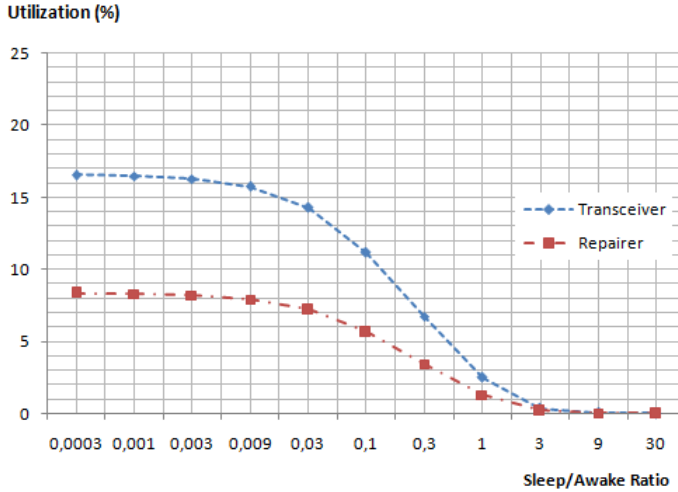


**FIGURE 13** Transceiver and repairer utilization versus Sleep/Awake ratio

432 Concerning the transceiver and the repairer utilization, we got the results depicted in Figure 13. It is clear that  
 433 in the fast configuration, we have a relatively great utilization for both of the transceiver (average of 15%) and the  
 434 repairer (average of 8%) in comparison to the fast part (very small percentage of utilization).

435 **6.2.3 | Influence of retrial rate**

436 When an SN does not find an idle neighbor to communicate with it, it has to wait a little bit before doing another  
 437 sending attempt so as not to exhaust its energy. This waiting time defines the retrial rate (RR). By varying RR, we  
 438 obtained the following results:

439  
 440 Figure 14 describes its impact on the mean battery charge. As expected, if RR increases, the mean battery charge  
 441 decreases. But when RR reaches the value 0.16 the mean battery charge stabilizes at the value 32.5% which is greater  
 442 than the go-to-sleep barrier by more than 20%. Therefore, if the network application requirement can afford a smaller  
 443 mean battery charge value, we can then use a smaller threshold.

444  
 445 Figure 15 illustrates RR's impact on the mean response time. As expected, when the time between two attempts  
 446 is tightened, the mean response time decreases. However, starting from the RR value 1.5, there is no mean response  
 447 time improvement. Therefore, increasing RR above this value and expecting to get a faster network, will be a complete  
 448 waste of energy.

449 Figure 16 depicts the use of the transceiver for several RR values. We notice that the more we tighten the time  
 450 between call attempts, the more we use the transceiver, because it is the main responsible of the sending process.

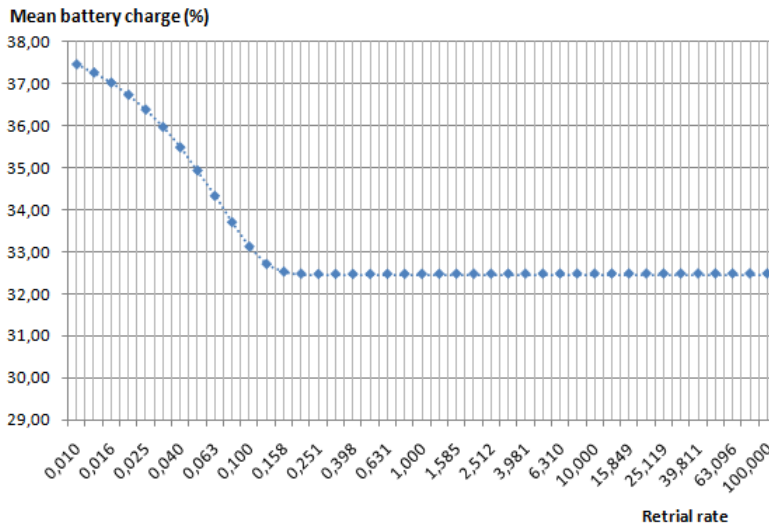


FIGURE 14 Mean battery charge versus retrial rate

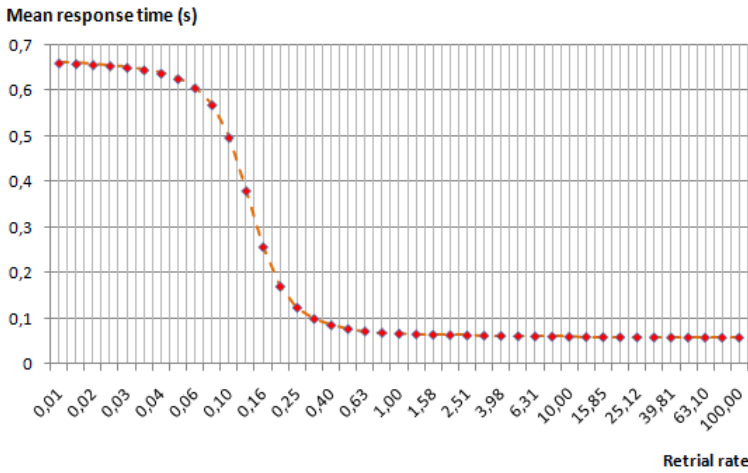
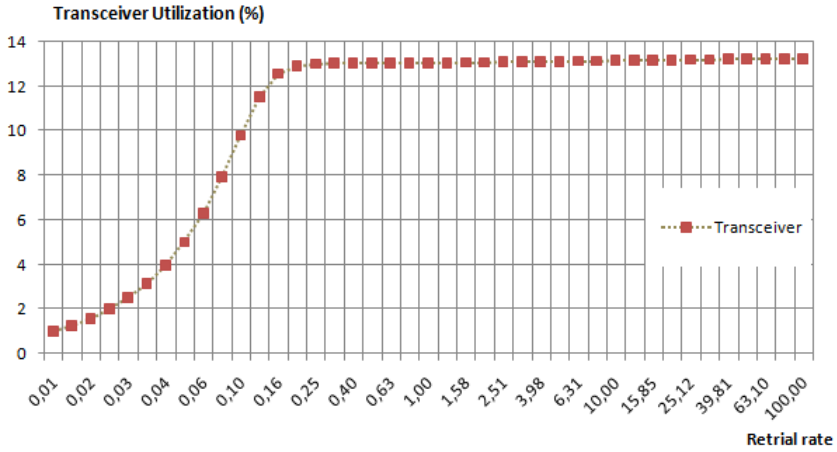


FIGURE 15 Mean response time versus retrial rate

451 However, the utilization gain stops short at the value 13.2% because abusing with retrial attempts exhausts the battery,  
 452 and the sensor will directly flip into a sleeping state where it won't be able to send anymore.

453 **6.2.4 | Influence of failures rate**

454 SN breakdowns phenomenon is an undesirable feature because it hinders the performance of the network. We can  
 455 partially cope with it by avoiding the reason of failure. In WSNs, most breakdowns stem from the expiration of battery  
 456 charge. Therefore, harvesting energy form the ambient involves a decrease of breakdown probability, which enhances



**FIGURE 16** Transceiver utilization versus retriail rate

457 the overall network performance. By changing the failure rate (FR) we got the following results:

458

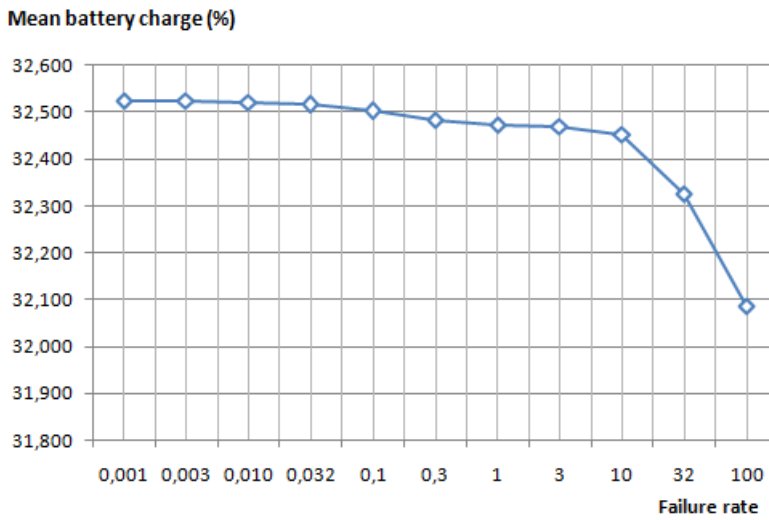


**FIGURE 17** Mean battery charge versus failure rate

459 Figure 17 allows us to study the FR effect on the mean battery energy. Broadly speaking, when FR increases, the  
 460 mean battery charge drops. Indeed, the SN not finding neighbors to forward its message, keeps attempting until it  
 461 succeeds. Furthermore, the busy breakdowns restart all the process of sending, which directly affects the amount of  
 462 energy stored in the battery.

463 Remember that in our modeling, we opted for the more general discipline of dependent breakdowns. That is, we



464 can have two kinds of breakdowns: active (busy) or idle, and their related probabilities are not necessary the same. In  
 465 addition, for the failure transition, we consider the strategy of infinite server, which means that each sensor may be  
 466 down independently from the others. Furthermore, we defined a threshold that prevents the SNs from exhausting  
 467 their batteries. In our experiments, we set  $T1$  to 20% and  $T2$  to 40%. For this reason, we can see in Figure 17 only a  
 468 small variation, when we increase FR.

469

470 Figure 18 illustrates the effect of FR on the mean response time. For example, if  $FR = 10^{-3}$ , which implies that  
 471 the neighbor battery charge drops to 20% between 3 and 4 times per hour, the mean response time nears 0.06 second.  
 472 We notice that for a relatively long delay between two breakdowns, the mean-response-time is very small. This later  
 473 remains stable at 0.06 second until FR reaches the value 10 where the mean-response-time starts to grow.

474

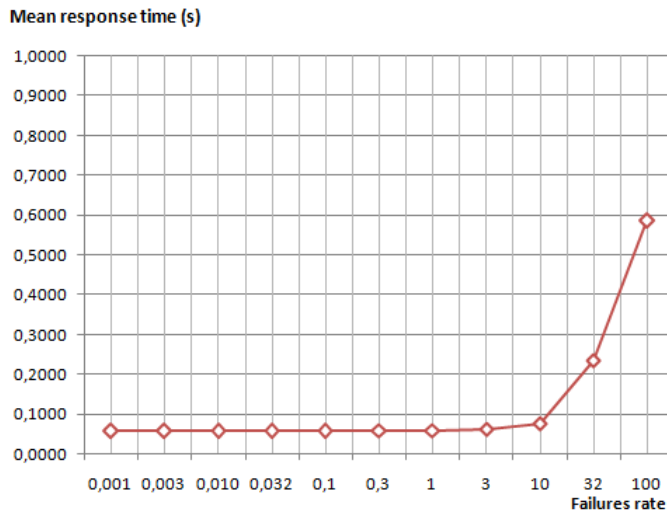


**FIGURE 18** Mean response time versus failures rate

475 Figure 19 depicts the behavior of the transceiver and the repairer. A high utilization of the transceiver (above  
 476 30%) is noticeable when FR is smaller than 0.3. In contrast to the transceiver behavior, the more there is breakdowns,  
 477 the more the repairer is solicited. We notice that the two curves intersect at an FR equal to 2. After this value, where  
 478 both utilizations of the transceiver and the repairer equal 10%, the situation is inverted.

479

## 480 6.2.5 | Influence of daily-message number

481 We analyzed the model by varying the daily number of messages (noted N) served by an SN. Figure 20 illustrates  
 482 the obtained results. We notice that the mean energy decreases when N increases until it reaches 73% for 300 daily  
 483 messages. Therefore, serving packets significantly affects the residual energy.

484 Further experiments can be conducted by considering other input parameters such as:

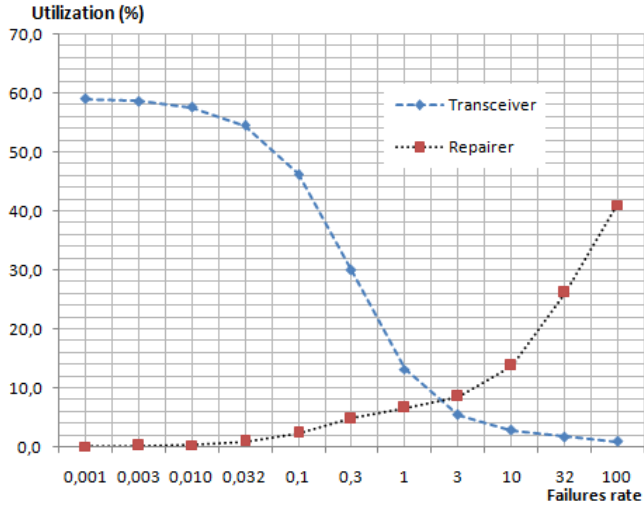


FIGURE 19 Transceiver and repairer utilization versus Failures rate

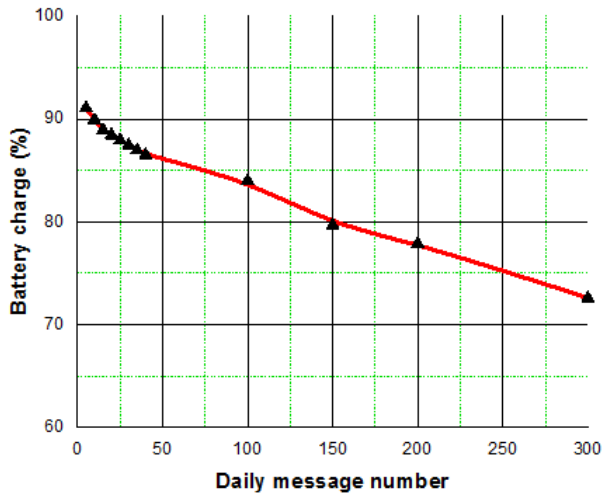


FIGURE 20 Mean battery charge versus daily message number

- 485 • Number of neighbors.
- 486 • Values of the two thresholds T1 and T2.
- 487 • Battery capacity.
- 488 • Number of neighbors.

### 489 6.3 | Case study

490 To further stress the proposed GSPN's ability to assess the feasibility and identify the requirements for setting a solar  
 491 energy harvesting WSN on an actual situation, we consider the case of deploying a network in the Algerian territory.  
 492 The utility of setting WSNs in Algeria which is the biggest country in Africa does not need to be proven. Indeed, in the  
 493 north, WSNs can be used, for example, to handle forest fires. In the south, they can be used to help fighting locust  
 494 invasion or for security concerns. Each of these possible applications has quite different requirements that govern the  
 495 feasibility of a network deployment.

496  
 497 Due to its geographical location, Algeria has one of the highest solar deposits in the world [45]. The duration of  
 498 insolation over almost the entire national territory exceeds 2000 hours annually and can reach 3900 hours (highlands  
 499 and Sahara). Figure 21 shows that the daily energy received on a horizontal surface of  $1m^2$  is of the order of 5 KWh  
 500 over most of the national territory, with nearly  $1700 KWh/m^2/year$  in the north and  $2263 kWh/m^2/year$  in the  
 501 south of the country.

502 A sensor equipped with a solar panel of  $10 cm^2$  can receive  $5wh$  per day. Table 5 shows features of the network we  
 503 consider in our case study.

504

**TABLE 5** Wireless sensor network case study features.

Parameter	Value
Mean number of neighbors for each SN	5
Sensor battery capacity	$5wh$
Mean daily message number	100
Surface of solar panel	$10Cm^2$

505 A message transfer consumes the highest amount of energy in comparison with other activities in the network  
 506 [7]. According to [46], a sensor consumes:

- 507 •  $3 mw$  in the active state (message sending).
- 508 •  $98 \mu w$  in the idle state.
- 509 •  $15 \mu w$  in the sleeping state.

510 The daily energy to be consumed by a sensor is the sum of the energies in idle state ( $E_i$ ), sleeping state ( $E_s$ ) and  
 511 active state ( $E_a$ ), such that:

$$E_i = \bar{\omega} \cdot \frac{1}{\theta} \cdot 98 \cdot 10^{-06} (wh) \quad (15)$$

512

$$E_s = \bar{\theta} \cdot \frac{1}{\omega} \cdot 15 \cdot 10^{-06} (wh) \quad (16)$$

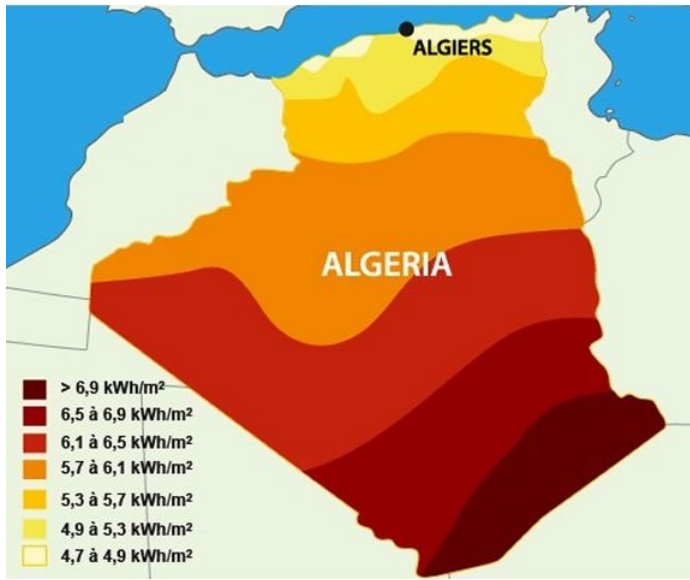


FIGURE 21 Algeria solar map [45]

513

$$E_a = \bar{R} \cdot N \cdot 3 \cdot 10^{-03} (wh) \tag{17}$$

514 Where:

515  $\bar{\omega}$  ,  $\bar{\theta}$  are the debits of the transitions *awake* , *Go\_sleep* given by eq.(10) and (11) respectively, and  $\bar{R}$  is given by  
 516 eq.(13).  $N$  is the mean number of messages per sensor and per day.

517 First, we define the parameter sleep/awake (SA) by the ratio (*sleeping delay/idle delay*). Figure 22 illustrates  
 518 the effect of SA on the mean response time. This later decreases when the sensors stay in idle state during a long  
 519 time aiming at serving messages upon their arrivals. Due to energy harvesting, we can increase the sensor listening  
 520 time in order to serve requests immediately, and consequently decrease the mean response time.

521 In order to show that our model allows to determine the suitable parameter (sleep/idle) delay ratio for each  
 522 territory, we vary the sleeping and the idle delays, and we calculate the daily energy consumption. Figure 23 shows  
 523 the daily energy consumption versus SA.

524 For example, if we configure the sensors in a way to stay one minute in the idle state and 8 minutes in the sleeping  
 525 state, then the daily energy consumption will be equal to  $5wh$ . This means that this configuration is appropriate to  
 526 the Sahara territory but not suitable for the north if we compare this result with figure 21 to ensure the liveliness of  
 527 the network. From the threshold  $7.6wh$ , the configuration becomes not suitable for any Algerian territory since the  
 528 biggest possible solar energy harnessing is  $7.2wh/m^2$  (see Figure 21 and note that  $kwh/m^2$  is equiv to  $wh/dm^2$ ).

529 One can argue that when the sensor is awake most of the time, it is supposed to consume more energy, but the  
 530 opposite is noticeable. Indeed, minimizing response time saves energy better than adopting a sleeping mechanism. It  
 531 is therefore important to keep the network's monitoring service awoken as long as possible.

532

533 Figure 24 represents the battery level status during one month for several values of the daily message number.

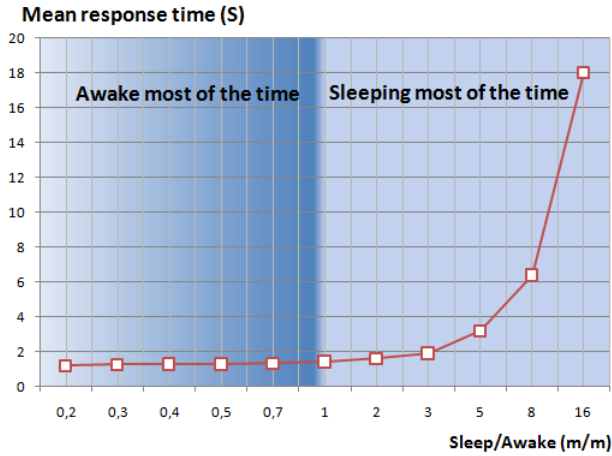


FIGURE 22 Mean response time versus sleep/idle ratio

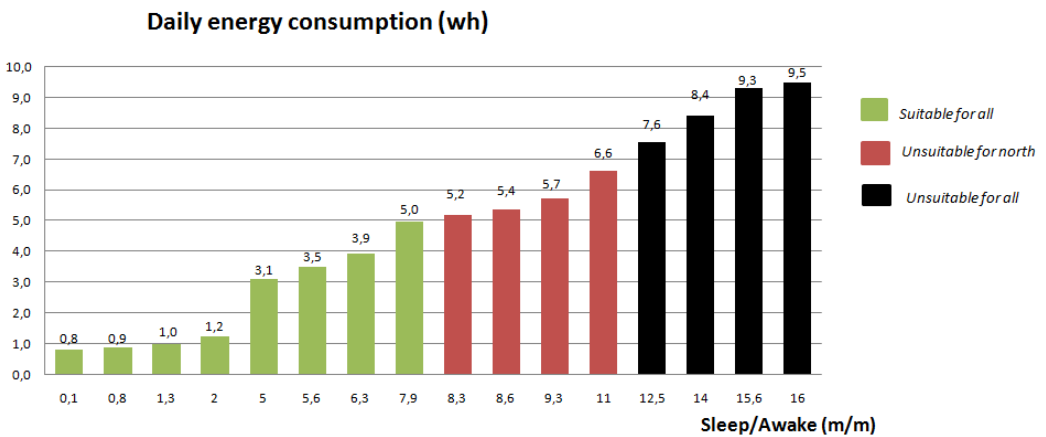
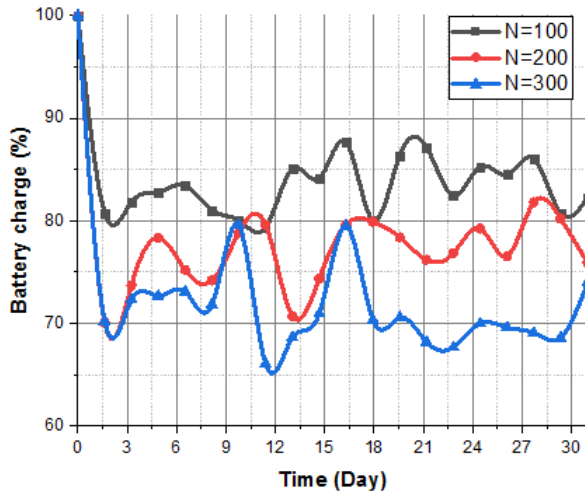


FIGURE 23 Daily energy consumption

534 We fed the model with the following values :

- 535 • Sleeping time: 2 minutes,
- 536 • Awakening time: 1 minute,
- 537 • Harvesting rate for Algiers province: 0.0139 quantum per second (one quantum /minute),
- 538 • Capacity: 100 quanta,
- 539 •  $T1 = 20\%$  and  $T2 = 40\%$ ,
- 540 • Neighbors number: 3,
- 541 • Working rate: 0.016 quantum per second,
- 542 • Retrial rate: 1,

- 543 • Active breakdowns rate:  $10^{-4}$ ,
- 544 • Idle breakdowns rate:  $10^{-6}$ ,
- 545 • Repair rate: 0.5,



**FIGURE 24** Battery charge versus daily message number during one month

546 This experiment shows the capability of the model to analyze different types of WSNs in terms of density and  
 547 number of served packets. We notice that the daily number of messages affects the energy level. For example, in the  
 548 case of a WSN with dense traffic ( $N=300$  messages per sensor and per day), the energy level is around 72%. Hence,  
 549 the selected configuration guarantees a continuous service for this WSN.

550  
 551 By setting the number of daily messages at ( $N = 100$ ), and by varying the number of neighbors ( $s$ ), we obtained  
 552 the results depicted in Figure 25. We notice that the number of neighbors does not affect the battery charge. It  
 553 seems that when the number of neighbors increases or decreases, it will affect the rapidity of the system instead of  
 554 the battery charge.

## 555 7 | CONCLUSION

556 In this paper, we proposed a Generalized Stochastic Petri Net to model the communication between a sensor and its  
 557 neighbors in a Wireless Network. The model takes into account different real aspects such as sleeping mechanism,  
 558 retrieval message attempts, battery recharge/discharge and battery-over breakdowns.

559 By using the TimeNet tool, several numerical results and diagrams are presented and discussed to show the influence  
 560 of different input parameters on the network performance.

561 A case study is given to analyze the requirements for installing a Wireless Sensor Network (WSN) in Algeria, by taking  
 562 into account the solar energy harvesting capabilities in different territories Algeria.

563 The proposed model proves to be able to address the trade-off between performance parameters and lifetime of sen-

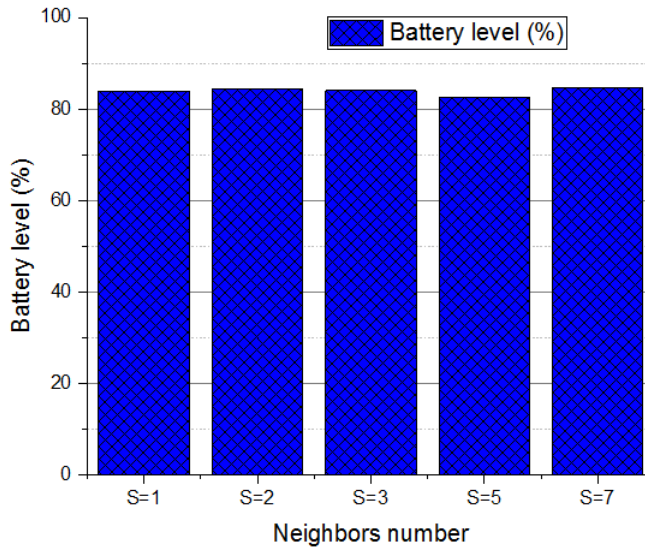


**FIGURE 25** Battery level versus neighbors number

564 sor nodes for deciding which input parameter to adjust in order to get the best performance of the Energy-Harvesting  
 565 WSN.

566

567 In our future works we will be focusing on including other important circumstances to our modeling, such as the  
 568 difference between message types, neighbor vicinity and sensor mobility.

## 569 references

- 570 [1] Basagni S, Naderi MY, Petrioli C, Spenza D. Wireless sensor networks with energy harvesting. *Mobile Ad Hoc Network-*  
 571 *ing: Cutting Edge Directions* 2013;p. 701–736.
- 572 [2] Kandris D, Nakas C, Vomvas D, Koulouras G. Applications of wireless sensor networks: an up-to-date survey. *Applied*  
 573 *System Innovation* 2020;3(1):14.
- 574 [3] Sudevalayam S, Kulkarni P. Energy harvesting sensor nodes: survey and implications. *IEEE Communications Surveys*  
 575 *and Tutorials* 2011;13(3):443–61.
- 576 [4] Ye W, Heidemann J, Estrin D. Medium access control with coordinated adaptive sleeping for wireless sensor networks. *IEEE/ACM Transactions on Networking (ToN)* 2004;12(3):493–506.  
 577
- 578 [5] Ali M, Böhm A, Jonsson M. Wireless sensor networks for surveillance applications—a comparative survey of mac proto-  
 579 *cols. IEEE; 2008. p. 399–403.*
- 580 [6] Ashraf N, Faizan M, Asif W, Qureshi HK, Iqbal A, Lestas M. Energy management in harvesting enabled sensing nodes:  
 581 *Prediction and control. Journal of Network and Computer Applications* 2019;132:104 – 117.
- 582 [7] Bahi J, Elghazel W, Guyeux C, Hakem M, Medjaher K, Zerhouni N. Reliable diagnostics using wireless sensor networks.  
 583 *Computers in Industry* 2019;104:103 – 115.

- 584 [8] Le K, Cao T, Le P, Pham B, Bui T, Quan T. Probabilistic congestion of wireless sensor networks: a coloured petri net  
585 based approach. *Communications on Applied Electronics* 2017;7(2):1–7.
- 586 [9] Younes OS. Modeling and performance analysis of a new secure address resolution protocol. *International Journal of*  
587 *Communication Systems* 2018;31(1):e3433.
- 588 [10] Zimmermann A. *Stochastic Discrete Event Systems Modeling, Evaluation, Applications*. Berlin, Heidelberg: Springer-  
589 Verlag; 2007.
- 590 [11] Oukas N, Boulif M. Sensor Performance Evaluation for Long-Lasting EH-WSNs by GSPN Formulation, Considering  
591 Seasonal Sunshine Levels and Dual Standby Strategy. *Arabian Journal for Science and Engineering* 2022;p. 1–15.
- 592 [12] Li J, Dai J, Issakhov A, Almojil SF, Souri A. Towards decision support systems for energy management in the smart  
593 industry and Internet of Things. *Computers & Industrial Engineering* 2021;161:107671.
- 594 [13] Shojafar M, Pooranian Z, Abawajy JH, Meybodi MR. An efficient scheduling method for grid systems based on a hierar-  
595 chical stochastic Petri net. *Journal of computing science and engineering* 2013;7(1):44–52.
- 596 [14] Shojafar M, Pooranian Z, Meybodi MR, Singhal M. ALATO: an efficient intelligent algorithm for time optimization in an  
597 economic grid based on adaptive stochastic Petri net. *Journal of intelligent manufacturing* 2015;26(4):641–658.
- 598 [15] Farooq MS, Idrees M, Rehman AU, Khan MZ, Abunadi I, Assam M, et al. Formal Modeling and Improvement in the  
599 Random Path Routing Network Scheme Using Colored Petri Nets. *Applied Sciences* 2022;12(3):1426.
- 600 [16] Shi L, Du S, Miao Y, Lan S. Modeling and performance analysis of satellite network moving target defense system with  
601 Petri nets. *Remote Sensing* 2021;13(7):1262.
- 602 [17] Azgomi MA, Khalili A. Performance evaluation of sensor medium access control protocol using coloured petri nets.  
603 *Electronic Notes in Theoretical Computer Science* 2009;242(2):31–42.
- 604 [18] Shi Zs, Wang Cf, Zheng P, Wang Hy. An energy consumption prediction model based on GSPN for wireless sensor  
605 networks. In: *2010 International Conference on Computational and Information Sciences IEEE*; 2010. p. 1001–1004.
- 606 [19] Yadollah zadehTabari M, Mohammadizad P. Modeling and Performance Evaluation of Energy Consumption in S-MAC  
607 Protocol Using Generalized Stochastic Petri Nets. *International Journal of Engineering* 2020;33(6):1114–1121.
- 608 [20] Lacerda B, Lima PU. Petri nets as an analysis tool for data flow in wireless sensor networks. In: *1st Portuguese Confer-*  
609 *ence on WSNs, Coimbra, Portugal Citeseer*; 2011. p. 1–6.
- 610 [21] Zairi S, Mezni A, Zouari B. Formal approach for modeling, verification and performance analysis of wireless sensors  
611 network. In: *International Conference on Wired/Wireless Internet Communication Springer*; 2015. p. 381–395.
- 612 [22] Bechar R, Tahar Abbes M, Mezzoudj F, Bellatreche L. On formal modeling and validation of wireless sensor network  
613 protocols. *Wireless Personal Communications* 2020;114(4):2855–2888.
- 614 [23] Dahiya R, Arora A, Singh V. Modelling the energy efficient sensor nodes for wireless sensor networks. *Journal of The*  
615 *Institution of Engineers (India): Series B* 2015;96(3):305–309.
- 616 [24] Bérczes T, Almási B, Kuki A, Sztrik J, Kakubava R. Modeling the performance and the energy usage of wireless sensor  
617 networks by retrial queueing systems. In: *Proceedings of the 8th ACM workshop on Performance monitoring and*  
618 *measurement of heterogeneous wireless and wired networks ACM*; 2013. p. 133–138.
- 619 [25] Wüchner P, Sztrik J, de Meer H. Modeling wireless sensor networks using finite-source retrial queues with unreliable  
620 orbit. In: *International Workshop on Performance Evaluation of Computer and Communication Systems Springer*; 2010.  
621 p. 73–86.



- 622 [26] Gharbi N, Charabi L. Wireless networks with retrials and heterogeneous servers: Comparing random server and fastest  
623 free server disciplines. *Int J Adv Networks Serv* 2012;5(1-2).
- 624 [27] Boutoumi B, Gharbi N. Two Thresholds Working Vacation Policy for Improving Energy Consumption and Latency in  
625 WSNs. In: *International Conference on Queueing Theory and Network Applications* Springer; 2018. p. 168-181.
- 626 [28] Oukas N, Boulif M. A petri net modeling for WSN sensors with renewable energy harvesting capability. In: *International  
627 Conference in Artificial Intelligence in Renewable Energetic Systems* Springer; 2019. p. 524-534.
- 628 [29] Oukas N, Boulif M, Hadiouche H, Bengharabi C. A New Petri Nets for WSNs to Model the Behaviour of Solar-Energy  
629 Harvesting Sensors with Double Sleeping Strategy. In: *2022 2nd International Conference on Computing and Informa-  
630 tion Technology (ICCI) IEEE*; 2022. p. 237-242.
- 631 [30] Oukas N, Boulif M. A New Generalised Stochastic Petri Nets Modelling for Solar Energy Harvesting Sensors in Long  
632 Lasting WSNs, Considering Seasonal Sunshine Levels. In: *Proceedings of The International Conference on Advances in  
633 Communication Technology, Computing and Engineering (ICACTCE) Meknes, Morocco*; 2021. .
- 634 [31] Oukas N, Boulif M. Generalized Stochastic Petri Nets Modelling for Energy Harvesting WSNs considering Neighbors  
635 with different Vicinity Levels. In: *2020 International Conference on Computing and Information Technology (ICCI-  
636 1441) IEEE*; 2020. p. 1-5. 10.1109/ICCI-144147971.2020.9213781.
- 637 [32] Oukas N, Boulif M. A Colored Petri Net to Model Message Differences in Energy Harvesting WSNs. In: *Proceedings  
638 of The 4th Conference on Computing Systems and Applications Ecole Militaire Polytechnique - Chahid Abderrahmane  
639 Taleb (EMP), Algiers, Algeria*; 2020. .
- 640 [33] Oukas N, Boulif M. Modeling and Assessment of Energy Harvesting WSNs with Unreliable Sensors for Military Appli-  
641 cations. In: *International Conference on Autonomous Systems and their Applications (ICASA 22), University of Eltaref-  
642 Algeria*; 2022. .
- 643 [34] Murata T. Petri nets: Properties, analysis and applications. *Proceedings of the IEEE* 1989;77(4):541-580.
- 644 [35] Peterson JL. *Petri net theory and the modeling of systems* 1981;.
- 645 [36] Marsan MA, Balbo G, Conte G, Donatelli S, Franceschinis G. *Modelling with generalized stochastic Petri nets*. John  
646 Wiley & Sons, Inc.; 1994.
- 647 [37] Florin G, Fraize C, Natkin S. Stochastic Petri nets: Properties, applications and tools. *Microelectronics Reliability*  
648 1991;31(4):669-697.
- 649 [38] Baccelli F. Ergodic theory of stochastic Petri networks. *The Annals of Probability* 1992;p. 375-396.
- 650 [39] Shaikh FK, Zeadally S. Energy harvesting in wireless sensor networks: A comprehensive review. *Renewable and Sus-  
651 tainable Energy Reviews* 2016;55:1041 - 1054.
- 652 [40] Mandru NP. Optimal power management in wireless sensor networks for enhanced life time. *Journal of Global Research  
653 in Computer Science* 2012;3.
- 654 [41] Almási B, Roszik J, Sztrik J. Homogeneous finite-source retrial queues with server subject to breakdowns and repairs.  
655 *Mathematical and Computer Modelling* 2005;42(5-6):673-682.
- 656 [42] Roszik J, Sztrik J. Performance analysis of finite-source retrial queues with nonreliable heterogenous servers. *Journal  
657 of Mathematical Sciences* 2007;146(4):6033-6038.
- 658 [43] Gharbi N, Ioualalen M. GSPN analysis of retrial systems with servers breakdowns and repairs. *Applied Mathematics and  
659 Computation* 2006;174(2):1151-1168.

- 660 [44] Zimmermann A. Modelling and performance evaluation with TimeNET 4.4. In: International Conference on Quantitative  
661 Evaluation of Systems Springer; 2017. p. 300–303.
- 662 [45] Yaiche M, Bouhanik A, Bekkouche S, Malek A, Benouaz T. Revised solar maps of Algeria based on sunshine duration.  
663 Energy Conversion and Management 2014;82:114–123.
- 664 [46] Hurni P, Braun T. Calibrating wireless sensor network simulation models with real-world experiments. In: International  
665 Conference on Research in Networking Springer; 2009. p. 1–13.